CZECH TECHNICAL UNIVERSITY IN PRAGUE
Faculty of Mechanical Engineering
Department of Process Engineering

MASTER THESIS

CFD Analysis of a Particulate Flow

Author: Malav Soni

Supervisor: Doc. Ing. Petera Karel Ph.D.

Prague, 2019

Statement

I declare that I have worked out this thesis independently assuming that the results of the thesis can also be used at the discretion of the supervisor of the thesis as its co-author. I also agree with the potential publication of the results of the thesis or of its substantial part, provided I will be listed as the co-author.

Prague, ...

                                                                Malav Soni

Annotation sheet

Name: Malav

Surname: Soni

Title Czech: CFD analýza toku partikulární látky

Title English: CFD analysis of a particulate flow

Scope of work: number of pages: 57

number of figures: 25

number of tables: 13

number of appendices: 3

Academic year: 2018 - 2019

Language: English

Department: Process Engineering

Specialization: Process Engineering

Supervisor: Doc. Ing. Petera Karel Ph.D.

Reviewer:

Tutor:

Submitter: Malav Soni

Annotation - English: Make a review of available approaches for particulate flows in ANSYS Fluent. Propose possible procedures for estimating particulate properties and try to find out realistic values. Evaluate the impact of time step on the results. Perform numerical simulations of particulate flow in a rotary kiln. Summarize the methodology used in the thesis and propose possible improvements of the solution procedure.

Keywords: DEM, KTGF, DDPM, particulate flow, multiphase, coefficient of restitution, spring-dashpot, correlation, Nusselt, rotating kiln

Utilization: For department of Process Engineering in Czech Technical University in Prague.

Abstract

In this study, CFD analysis of a particulate flow inside rotating kiln has been carried out. For this analysis purpose, ANSYS Fluent software is used. ANSYS Fluent offers various models for simulation of particulate flow and these models require various parameters to model behavior of continuous phase flow and dispersed phase flow. In this study, evaluation of time step, coefficient of restitution, spring constant and static frictional coefficient has been carried out.

Inside rotating kiln, analysis of heat transfer between continuous phase and discrete phase has been modelled. There are many factors that can affect this heat transfer. These factors have been discussed in this study. A correlation describing heat transfer between particles and hot gas in a given geometry of rotating kiln was evaluated.

Acknowledgements

First, I want to express my deepest gratitude to Professor Petera Karel, for his supervision, support and guidance throughout my work on this thesis.

I am grateful to my father, Dr. Sudhir Kumar Soni, my mother, Rita Soni and my sister, Deval Soni for giving me support every time I needed and standing beside me at every important moments of my life.

I want to thank Czech Technical University for giving me this opportunity to study in the beautiful city of Prague.

Table of Contents

List of Figures

List of Tables

1. Introduction

Multiphysics coupling between the laws that describe fluid dynamics and structural mechanics is known as fluid structure interaction. Particulate flow is one of the many branches of fluid structure interaction, which consists of at least two different phases where one phase considered as discrete or dispersed phase stays in contact with continuous phase. Generally continuous phase is gas or liquid phase and dispersed phase can be solid, liquid or gas particles, droplets or bubbles. For example, sand and moisture particles in air, fish tank model, propagation of aerosol particles in air, etc. This study is focused on particulate flow of solid particles in some rotating kiln and heat transfer between these solid particles and hot gas flowing through rotating kiln. There are many various parameters like size, mass and density of these particles, velocity of hot gas, angular velocity of kiln, and physical properties of particle, gas and wall of kiln materials that can affect the heat transfer. Therefore, it is not analytically possible to evaluate this heat transfer and one must use an approach based on real experiments, or numerical simulations based on CFD (Computational Fluid Dynamics).

When it comes to numerical analysis of particulate flow, ANSYS Fluent is one of the many CFD software available in market. ANSYS Fluent offers number of models to solve particulate flow problem. These models are divided into main two types. First is Euler-Euler models and second is Euler-Granular models. In E-E models, both continuous phase and discrete phase are tracked in the Eulerian reference frame while in E-G models, the continuous phase is tracked in the Eulerian reference frame and discrete phase is tracked in the Lagrangian reference frame. Selection of these model for any specific simulation mainly depends on balance between accuracy of model that is to be simulated and required time to run that said simulation.

2. Objectives

Make a review of available approaches for particulate flow in ANSYS Fluent: As mentioned earlier, there are number of models (approaches) through which we can solve problem of fluid structure interaction. Selection of a model for given problem will depend on definition and parameters of problem. In this case, the given problem is to simulate heat transfer between particles and hot gas inside rotating kiln.

Evaluation of ideal size of time step: In ANSYS Fluent, time step represents incremental change in time for which the governing equations are being solved. In other words, time steps are used to advance the calculation in real time by small fraction of time. During the solution of cases like particulate flow, standard procedure is, calculation of continuous phase flow field at an instance of time and then evaluation of particle trajectories and then redoing same calculation by updating source terms for next instance of time. As there are different models to solve particulate flow problem, the ideal length of time step will be different for each model and it can have substantial impact on the results. The smaller is the time step, the better is the accuracy, but the computational requirements increase on the other side – therefore it is important to find out some optimal value of the time step.

Evaluation of Nusselt relation for heat transfer between hot fluid and solid particles: In rotating kiln, heat transfer between hot gas and cold solid particles can be affected by many parameters such as speed of angular velocity of kiln, velocity of hot gas, size and shape of baffles inside kiln, etc. This study will also try to evaluate how heat transfer changes due to change in velocity of gas and angular velocity of kiln.

Relation between Nusselt number and Reynold's number: Number of different relations between Nusselt number and Reynold's number are proven in different research papers. In this study I will also try to evaluate this relation and see if it is affected by change in various parameters like rotation speed of kiln and velocity of gas phase.

3. Multiphase Flow

Before going directly to the topic of this study, there are some basic terms, which must be explained to make understanding of procedure and analysis of results easy.

3.1 Types of Reference Frames

Lagrangian reference frame: In classical physics, the Lagrangian reference of the field is a way of studying a fluid motion where the observer follows an individual fluid parcel as it moves through space and time. When the position of this parcel is plotted against time, it gives the path line of fluid. This can be visualized as sitting in a boat and observing a parcel of fluid as it flows down the river along with boat.

Eulerian reference frame: The Eulerian reference of the flow field is a way of studying a fluid motion that focuses on specific locations in the space through which the fluid flows as time passes. This can be visualized by sitting on the bank of a river and observing the flowing water at a fixed location.

These reference frames are important in computational fluid dynamics where Eulerian reference frame employs a fixed mesh while Lagrangian reference frame deals with parcels that may move according to the velocity field.

ANSYS offers two basic types of numerical solution approach in terms of multiphase flow. One is called Euler-Euler approach and other is called Euler-Lagrangian approach.

In the Euler-Euler approach, there are three models to simulate a multiphase flow: the volume of fluid (VOF), the mixture model and the Euler model. Here, the primary phase which is continuous phase is treated by solving the time-averaged Navier-Stokes equations. While the behavior of secondary phase (dispersed phase) is evaluated by tracking a large number of particles through the calculated continuous phase frame. Dispersed and primary phases can exchange mass, momentum and energy (Kozic et al., 2011).

The second approach that is Euler-Lagrangian approach, where the continuous phase is treated in an Eulerian reference frame and is evaluated by solving the time-averaged Navier-Stokes equations and the dispersed phase is solved by computing the trajectories of a large number of particles by numerically integrating the equations of motion for the discrete phase throughout the flow domain. Here, the dispersed phase is considered as point masses consisting of spherical particles which do not displace the continuous flow field. This dispersed phase can exchange energy, mass and momentum with the fluid phase. The effect of continuous phase on dispersed phase is calculated through drag models and turbulence models, however

vice versa effect can be considered or neglected by changing the condition of coupling between discrete and continuous phase.

3.2 Phase Coupling

In ANSYS Fluent, ways of phase coupling describe that how a change in one phase affect the motion and force exerted on the other phase. Before going into phase coupling, there are some fundamental definitions related to phase coupling, which must be explained.

Dilute Flow: When the motion of dispersed phase is controlled by the forces of continuous flow field such as drag and lift force, it is called as dilute flow.

Dense Flow: When the motion of dispersed phase is controlled by collision between particles, it is called as dense flow. Dense phase is further divided into two parts:

1. Collision dominated flow: In collision dominated flow, the collision between the particles control the features of the flow. For e.g. particles in fluidized bed
2. Contact dominated flow: When the motion of dispersed phase is controlled by continuous contact of particles such as in a shear granular flow.

Volume Fraction: The volume fraction of dispersed phase is defined as

$$\alpha_d = \lim_{\delta V \to V^0} \frac{\delta V_d}{\delta V} \tag{1}$$

Where δV_d is the volume of dispersed phase and V^0 represents the volume that ensures a stationary average.

The volume fraction of the continuous phase is defined as

$$\alpha_q = \lim_{\delta V \to V^0} \frac{\delta V_q}{\delta V} \tag{2}$$

Where δV_q is the volume fraction of the continuous phase. And according to the definition, the sum of all volume fractions for same system must be unity.

$$\alpha_d + \alpha_q = 1 \tag{3}$$

3.3 Types of Phase coupling

One-way coupling: when the forces of continuous field flow affects the motion of discrete particles, but there is no reverse effect, then it is one-way coupling.

Two-way coupling: If there is mutual effects of forces and momentum between both the phases then It is two-way coupling.

Four-way coupling: In addition to above two effects, if there is also particle-particle motion affecting the phase motion then it is four-way coupling.

One-way and two-way coupling are used for dilute flow. According to research, when volume fraction of dispersed phase is below 10^{-6} it is best to use one way coupling and when this volume fraction is between 10^{-6} to 10^{-3}, two-way coupling is used. When the volume fraction of dispersed phase is greater than 10^{-3} four-way coupling is used and as said earlier, this type of flow is called as dense flow. (Franziska at al, 2016)

This study covers the simulation of heat transfer inside rotating kiln between particles and gas. Therefore, it becomes the case of dense flow and the use of four-way coupling is necessary.

According to ANSYS Fluent, the model which provides such solution with Eularian-Lagrangian approach is called Dense Discrete Phase Model (DDPM). In this model, for continuous phase as said earlier, it is evaluated in an Eulerian reference frame by solving the time-averaged Navier-Stokes equations. But, for particle-particle interaction, there are two theories in DDPM model. One is Kinetic theory of granular flow (KTGF) and the second is Discrete Element Method (DEM).

3.4 DDPM-KTGF

Kinetic theory of granular flow describes large number of submicroscopic particles, all of which are in constant rapid and random motion. The randomness arises from the collisions with each other and with walls of the container. Hence, the approximate interactions are calculated.

The continuity for particulate phase is given by following equation:

$$\frac{\partial}{\partial t}(\alpha_d \rho_d) + \nabla.(\alpha_d \rho_d \overrightarrow{u_d}) = 0 \qquad (4)$$

And the particulate phase momentum balance must include drag model, virtual mass force and lift force. The solid pressure and solid stress tensor terms are modeled based on the theory of granular flows, as described by Gidaspow et al., 1992 as well as Ding and Gidaspow (Ding at al., 1990). The granular temperature is obtained using an algebraic equation (Syamlal at al., 1993.) Momentum balance for particulate phase is given as follows:

$$\frac{\partial}{\partial t}(\alpha_d \rho_d) + \nabla \cdot (\alpha_d \rho_d u_d u_d) = -\varepsilon_d \nabla p - \nabla p_d + \nabla \cdot \overrightarrow{\tau_d} + \varepsilon_d \rho_d g$$

$$+ \beta(u_q - u_d) + F_{vm} + F_{lf} \qquad (5)$$

Generally, computations are comparatively faster with KTGF method than DEM method due to modelling of particle interaction effect.

3.5 DEM

The Discrete Element Method (DEM) was originally proposed by Cundall and Strack, 1979. In this method, for particle-particle interaction, soft sphere approach is used, where it is assumed that two particles can have some deformation after they collide. These deformations are measured by an overlap displacement with respect to the ideal particle size. The soft-sphere model allows the possibility to have one particle in contact with more than one other particles. In DDPM-DEM model, for continuous phase, as mentioned earlier, time-averaged Navier-Stokes equation is solved and for particle motion, following equation is used: (Debashis et al, 2015)

$$m\frac{d\overrightarrow{u_d}}{dt} = \vec{F}_{drag} + \vec{F}_{pressure} + \vec{F}_{virtual\ mass} + \vec{F}_{gravitation} + \vec{F}_{other} + \vec{F}_{\delta}$$

$$+ \vec{F}_{friction} \qquad (6)$$

where the term $\vec{F}_{\delta}$ and $\vec{F}_{friction}$ depends on the method of contact force calculation

There are several ways to calculate these contact forces. Basic ones are linear Spring force model and linear Spring-Dashpot model, in which contact forces are calculate in normal direction and Fluent laws of friction can be applied to calculate forces in tangential direction. In ANSYS fluent, following contact force laws are used:

- Spring
- Spring-Dashpot
- Friction

Spring collision law: For spring collision law as unit vector is defined as $\overline{e_{12}}$ from particle 1 to 2. The force on particle 1 ($\bar{F}_1$) can be calculated using a spring constant.

$$\bar{F}_1 = K\delta\overline{e_{12}} \tag{7}$$

$$\bar{F}_1 = -\overline{F_2} \tag{8}$$

Where, δ represents overlapping of particles during collision.

The spring-Dashpot collision law: For spring-dashpot law, a spring constant K is defined as previous law and also a coefficient of restitution ν is defined where $0<\nu<=1$. If material is perfectly elastic, then $\nu =1$.

For collision calculation with this law, following equations are evaluated: (Branco et al, 2015)

Loss factor: $\qquad\qquad f_{loss} = \sqrt{\pi^2 + \ln^2\nu}$

Reduced mass: $\qquad\quad m_{12} = \frac{m_1 m_2}{m_1 + m_2}$

Collision time scale: $\quad t_{coll} = f_{loss}\sqrt{\frac{m_{12}}{K}}$

Damping coefficient: $\quad \gamma = -2\frac{m_{12}\ln\nu}{t_{coll}}$

With these expressions, the force on particle 1 can be defined as,

$$\bar{F}_1 = \left(K\delta + \gamma(\bar{v}_{12} \cdot \bar{e}_{12})\right)\bar{e}_{12} \tag{9}$$

From this value of $\bar{F}_1$, according to equation (8), value of $\overline{F_2}$ can be calculated.

The friction collision law: The friction collision law is based on the law of coulomb friction,

$$\bar{F}_{friction} = \mu\bar{F}_{normal} \tag{10}$$

Where, μ is the coefficient of friction and $\bar{F}_{normal}$ is the force normal to the surface.

Parcels: When using the discrete phase model in ANSYS Fluent, it is often required to input mass flow rate of discrete particles. This mass flow rate is converted into

injected number of particles per unit time. But sometimes it happens that it is prohibitive to track all the particles when mass flow rate is large. To prevent loss of particle track in such cases, Fluent tracks number of 'parcels', and each parcel represents a fraction of total mass flow rate.

In DEM, the concept of parcels is important. When the parcels occupy a finite volume and interact with other parcels, the volume occupied by a parcel is calculated from the mass of particles that parcel represents, hence it has same density as a particle. Therefore, while calculating the particle-particle interaction and forces, parcel diameter is used, but for trajectories of particles (or parcels) through a fluid domain, particle diameter is used.

ANSYS Fluent offers four types of parcel release method: Standard, constant-number, constant-mass and constant-diameter. Number of parcels is determined accordingly from the given injection mass flow rate.

3.6 Turbulence model

In some cases of multiphase flow, especially where one phase is continuous phase and other phase is dispersed phase, it is necessary to include turbulent model. There are various models available to describe the turbulent fluctuations of velocity and scalar quantities of a flow. The number of terms to model in a multiphase momentum equation for a turbulent model is large, therefore the modeling of turbulence in a multiphase flow is complex.

According to ANSYS Fluent there are three basic approaches to calculate a turbulent flow.

- Direct Numerical Simulation (DNS)
- Large Eddy Simulation (LES)
- Reynolds Averaged Navier-Stokes Simulation (RANS)

Number of models are developed from each approach. "Realizable k-ε" model based on RANS is used for this study. In this model, time-averaged Navier-Stokes equations are solved.

Reynolds Averaged Navier-Stokes Simulation (RANS): In many engineering solutions, determining the structure of turbulence flow is not important but, it is enough to obtain main affecting flow quantities like wall shear stress, time averaged velocity, Nusselt number, etc.
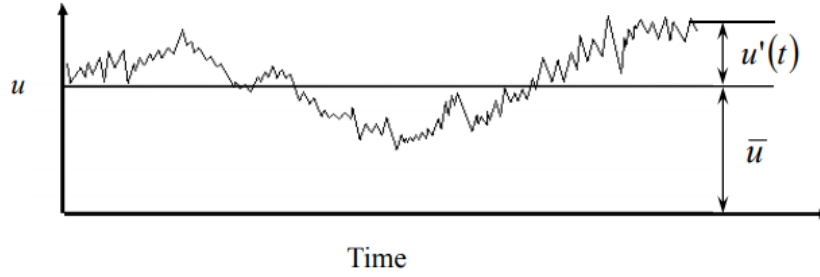
Figure 1: instantaneous velocity of fluid

At any instance of time, for a turbulent flow, according to Reynolds decomposition, $u = \bar{u} + u'$.

Where $\bar{u}$ is time averaged velocity and u' is fluctuating velocity. The value of this fluctuating velocity on averaged time must be zero.

After decomposition of the velocity components, it can be averaged over time with the help of Reynolds operators (Gian-Carlo, 1964) and can be rewritten as Reynolds-Averaged Navier-Stokes (RANS) equations:

$$\rho \left(\frac{\partial \bar{u}_i}{\partial t} + \bar{u}_k \frac{\partial \bar{u}_i}{\partial x_k} \right) = -\frac{\partial \bar{p}}{\partial x_i} + \frac{\partial}{\partial x_j} \left(\mu_l \frac{\partial \bar{u}_i}{\partial x_j} \right) + \frac{\partial R_{ij}}{\partial x_j} \qquad (11)$$

Here, R_{ij} is Reynolds stress tensor, $R_{ij} = -\rho \overline{u_i' u_j'}$ in which the turbulence effects are hidden. These stresses are additional unknowns which cannot solved analytically and must be modelled to close the system of governing equation. "Realizable k-ε" method is one of the closure models.

More detail about this model can be found in article "Turbulence in multiphase flow" by Besnard at al. (1988) or ANSYS Fluent Theory Guide.

4. Evaluation of Time Step

In ANSYS Fluent, it is needed to specify the length of the time step in a transient case. This time step determines real time advancement of simulation with each and every iteration. Size of time step does not only affect the accuracy of simulation, but it also affects the time taken to simulate the model for given "time" because, the smaller the time step size, a greater number of the time steps and iterations are required to simulate given real time. However, to model transient phenomena properly, it is necessary to set the time step size at least one order of magnitude smaller than the smallest time constant in the system being modelled.

According to ANSYS, a good way to judge the choice of time step size is to observe the number of iterations ANSYS Fluent needs to converge at each time step. The default number of iterations per time step is 20. If the size of time step is subsequently larger, then it will take more iteration per time step to converge to a solution.

4.1 Workbench setup for time step evaluation

As per standard procedure of CFD simulation, a fluid domain was created in ANSYS Design Modeler. The concept is to simulate a particle drop, in two-dimensional space with air as a continuous phase and anthracite particle as a discrete phase with default settings and evaluate the reflection height of first bounce of particle from wall as well as time taken to reach that height.

The 2D fluid domain has dimension of 200 mm x 500 mm rectangular shape and particle is dropped from height of 500 mm. It is well known that smaller mesh element size gives better accuracy of convergency but in case of Discrete Element Method (DEM), it is required to maintain particle size equal to or smaller than mesh element to prevent any issues with convergence. On the other hand, for DDPM with KTGF, it is required to set element size as minimum as possible. In my simulations, as I am comparing the results for both DEM and KTGF, mesh element size is kept at 5 mm with total number of 4000 elements. On next page, you can see the figure illustrating grid size of fluid domain for this setup.
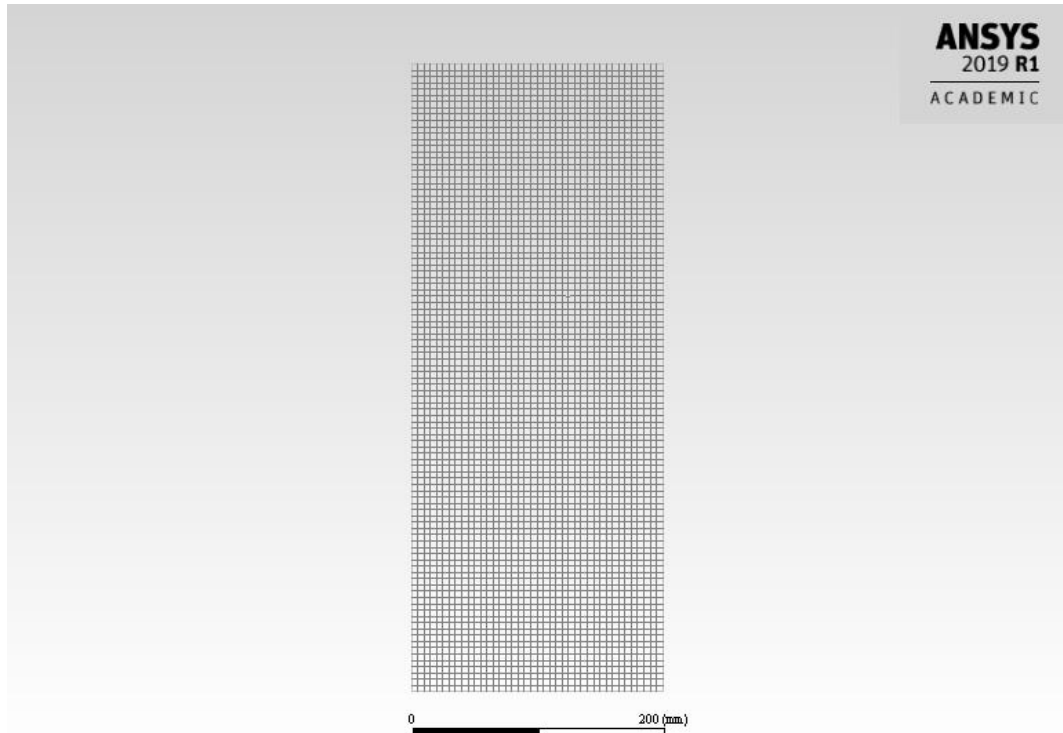
Figure 2: Fluid domain for particle drop test

Fluent requires us to give data for particle injection such as particle diameter, velocity, type of injection, starting and stopping time of injection, etc. Here are the injection parameters for given case.

Injection type:	Single
X position:	100 mm
Y-position:	495 mm
X-Velocity:	0 m/s
Y-Velocity:	0 m/s
Diameter:	5 mm
Flow rate:	3043.14 kg/s
Start time:	0 s
Stop time:	0.0001 s (for KTGF)
Stop time:	0.00001 s (for DEM)

Other settings are kept as default such as, type of discrete phase material is anthracite, and density is 1550 kg/m^3. Settings related to multiphase modelling and boundary conditions will be explained in later sections.

4.2 Analysis of Results

Simulations were performed for various time step size for both KTGF and DEM model and results were obtained for height of particle reflect and time taken to reach that

height. Below is the typical graph of particle height against time and table of time step size, height of first reflect and time.
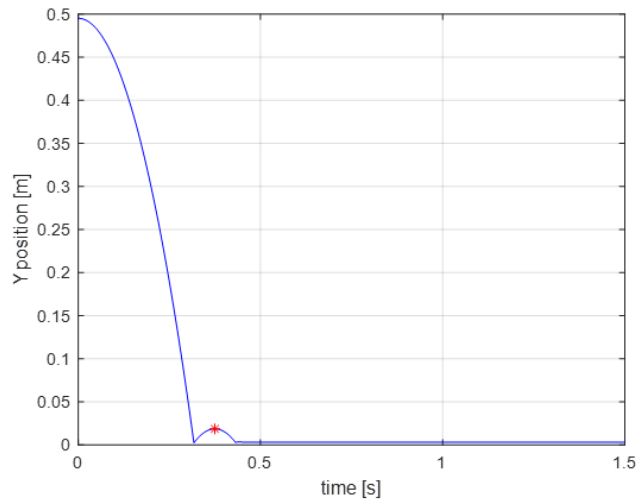
Figure 3: Typical graph of particle position v/s time

DEM

Time step size [s]	Height of first reflect [m]	Time taken [s]
0.005	0.016625	0.371734
0.001	0.016788	0.371145
0.00075	0.018697	0.374780
0.000625	0.018654	0.374707
0.0005	0.018675	0.374719
0.00025	0.018576	0.375677

Table 1: Change in height of first reflection of particle with time step in DEM

KTGF

Time step size [s]	Height of first reflect [m]	Time taken [s]
0.01	0.010840	0.365230
0.009	0.010894	0.366203
0.008	0.010895	0.366203
0.005	0.010872	0.366426
0.001	0.010797	0.364857
0.0008	0.010785	0.364800

Table 2: Change in height of first reflection of particle with time step in KTGF

Best way to find out the optimum size of time step is to calculate the deviation in height of first reflect at given time step from previous time step size. The calculation

procedure to evaluate this deviation is same as examining "Spatial (Grid) Convergence." This method is used to evaluate the discretization error in a CFD simulation.
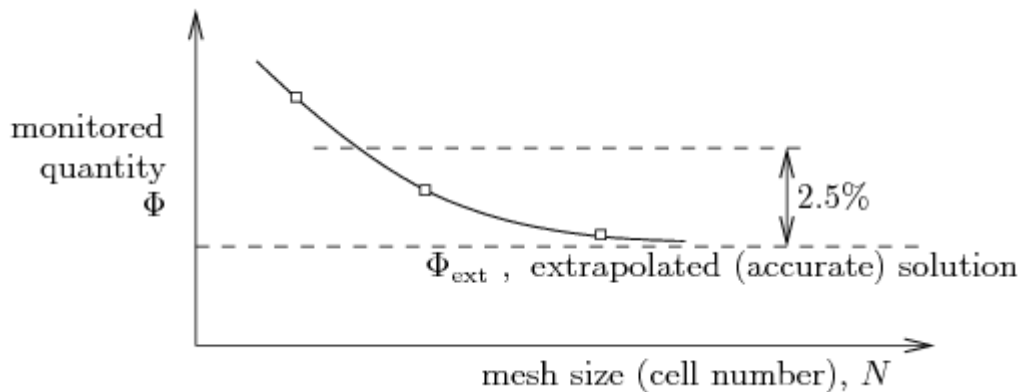
Figure 4: Spatial Convergence graph

In this method, the simulations are performed on two or more successively finer grids and discretization error for measured quantity is calculated by following equation,

$$\Phi = \Phi_{ext} + aN^{-p}/_{D} \tag{12}$$

In this equation, N represents the number of mesh elements, D will be 2 in case of 2-D case and 3 in case of 3-D case. When examining the time step convergency, it represents 1-D problem, hence for this calculation, D is 1. Now, there are three unknowns, Φ_{ext}, a and p. These unknowns can be calculated from three different equations from measured quantity for given mesh size. (see Celik et al., 1993) Here, Φ_{ext} refers to the value of measured quantity at infinite number of mesh element.

Similar way, we can calculate for the time step size error by replacing number of mesh element to time step size and measured quantity will be height of reflection. I have attached a MATLAB script in the appendices to calculate an extrapolated value with error of accuracy.

This MATLAB script will calculate error of accuracy for given three time step sizes in percentage and will plot these value in a graph. Below is the graph of height of reflect (measured quantity) against number of time step for 1 second simulated time and table for error in accuracy for DEM.
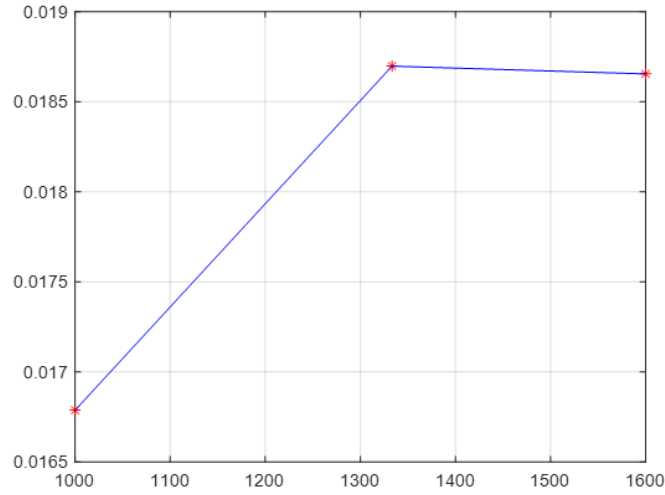
Figure 5: Height of reflection v/s number of time steps for DEM

Time step size (s)	Number of time step for 1 second	Error in accuracy (%)
0.000625	1600	0.027
0.00075	1333	0.27
0.001	1000	13.86

Table 3: Accuracy error in particle reflection height for given time step size in DEM

From above results, ideal time step would be 0.00075 s as it has only 0.27% error in accuracy of result.

Ideal time step size for DDPM-KTGF is also evaluated by same method.
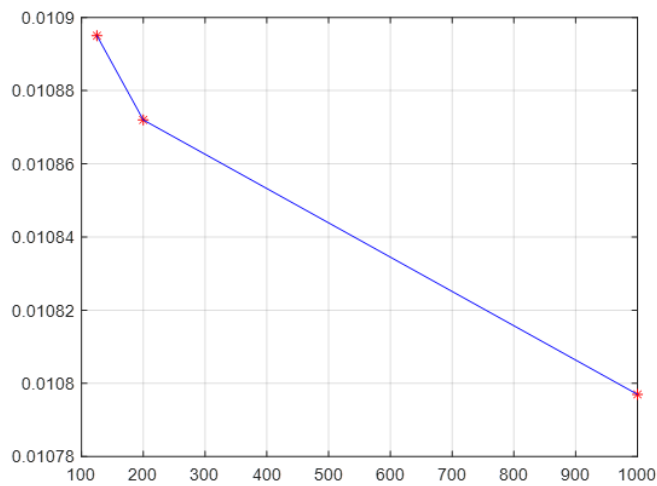
Figure 6: Height of reflection v/s number of time steps for KTGF

22

Time step size [s]	Number of time step for 1 second	Error in accuracy (%)
0.005	125	0.042
0.008	112	0.18
0.009	100	2.95

Table 4: Accuracy error in particle reflection height for given time step size in KTGF

From this result, we can consider that the time step size 0.008 s with 0.18 % accuracy is ideal time step size for a multiphase flow with particle-particle interactions based on the kinetic theory of granular flow.

5. Evaluation of Particle Collision Parameters

In ANSYS Fluent, to simulate a multiphase flow with particle-particle interaction, we must provide some data to the Fluent solver which can reflect the behavior of these particles. In this case these data are coefficient of restitution, spring constant and coefficient of friction. Experiments were performed in lab for a particle material which was given to me by my supervisor and it is the same material that goes into rotating kiln in real operations. It corresponds to the material in the final stage of production.

5.1 Coefficient of Restitution and Spring Constant

As mentioned earlier, that coefficient of restitution is required in both DEM and KTGF to calculate particle-particle interactions, especially for KTGF where only coefficient of restitution is used to model particle reflection in normal direction.

Coefficient of restitution is the ratio of final velocity to the initial velocity between two objects after they collide.

$$Coefficient\ of\ Restitution\ (v) = \frac{V_2}{V_1}$$

Experimental Data: The concept to evaluate coefficient of restitution from experiment is, the given particle should be dropped from a specific height and then measure the height of the reflection (bounce from ground). Similar setup can be created in ANSYS Fluent and with different restitution coefficient, different particle reflection height can be measured, and the results can be compared.

As mentioned above, particle material was provided by my supervisor with following property:

Mass: 0.1126 g
Average diameter: 7.8 mm
Volume: 248.4748 mm³
Density: 453.1647 kg/m³

After performing this experiment 10 times by dropping the particle from 50cm height, following results were obtained:

Time of impact to the ground [s]	Time at which particle reaches max height after bounce [s]	Height of bounce [cm]
1.308	1.906	11.72
1.221	1.653	7.727
1.033	1.474	2.333
1.140	1.200	5.022
1.149	1.383	3.033
1.091	1.456	4.5
1.066	1.460	4.884
1.036	1.737	16.7045
1.027	1.560	11.4545
1.069	1.618	3.9215

Table 5: Height of first reflection of a real particle

Here we can see that not all the experiments give same result, that is because of irregularity in shape of particle. Therefore, it is necessary to consider average height of bounce. This average height is 7.130 cm.

Simulation Data: Simulations were performed for this setup in ANSYS Fluent with different coefficient of restitution for KTGF and for DEM with different combinations restitution coefficient and spring constant. Unlike previous simulations, before beginning the simulations, it is necessary to change the density of particle material to real particle density. In both the cases, particle is injected at 50cm height.

KTGF:
 Here is the result of simulation with KTGF model having different coefficient of restitution and graph of height of refection against coefficient of restitution. Notice the increase in the height of particle reflection with increase in the value of restitution coefficient.
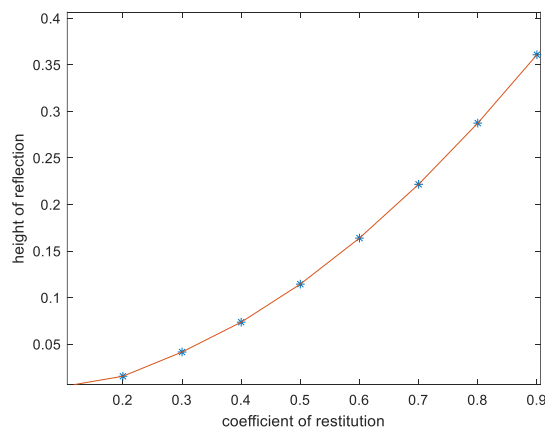
Figure 7: change in height of reflection with v for KTGF

ν	Height of reflection [m]
0.1	0.004645
0.2	0.015535
0.3	0.041571
0.4	0.073605
0.5	0.114451
0.6	0.163875
0.7	0.221615
0.8	0.287345
0.9	0.360733

Table 6: Height of reflection for given value of ν for KTGF

Value of ν can be evaluated for calculated experimental height of bounce that is 0.0713 m using following MATLAB command:

```
nu_y=interp1(y,nu,0.07129,'PCHIP')
```

This gives ν= 0.3936.

DEM:

For DEM, I have used spring-dashpot contact force law in normal direction, for that I need value of two parameters which are coefficient of restitution and spring constant. In DEM it is tricky to evaluate these parameters because with increase in coefficient of restitution from 0 to 1, height of particle reflection will increase but with increase in spring constant, height of particle reflection will decrease as particle will tend to achieve rigidity. Hence, there will be infinite number of combinations of spring constant and coefficient of restitution for given height of particle reflection. It is recommended by ANSYS that, if the value of spring constant is not known then we should take it from the range of 100 to 1000 N/m. Simulations were carried out for spring constant 100, 500 and 800 N/m with coefficient of restitution ranging from 0 to 1. Below we can see the graph of height of particle reflection against restitution coefficient for K = 100 N/m.
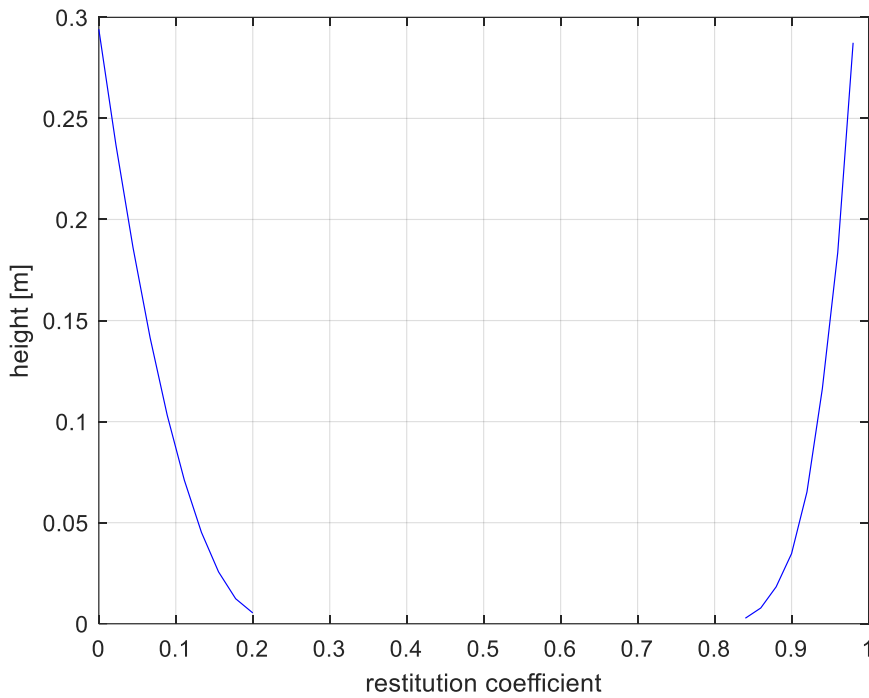
Figure 8: Graph of coefficient of restitution v/s height for K=100 in DEM

From above graph it is clear that for spring-dashpot contact law, for given spring constant, the relation between height of particle reflection and restitution of coefficient is first decreasing and then increasing in nature and instead of one, there can be two possible solutions for coefficient of restitution for the given height of particle reflection and spring constant.

In the table below, we can see the two values of restitution coefficient to achieve 0.0713m height of particle reflection for K = 100, 500 and 800 N/m.

K [N/m]	v_1	v_2
100	0.111	0.923
500	0.449	0.923
800	0.498	0.891

Table 7: Combinations of K and v for given height of particle reflection

5.2 Evaluation of coefficient of static friction:

It is necessary to evaluate the coefficient of friction especially between particle and wall of rotating kiln because, we want particles to travel across the kiln length and calculate particle residence time, which will be greatly affected by friction between particles and wall of kiln. A simple experiment was performed to evaluate this coefficient of friction. The wall material for rotating kiln was provided to me by my thesis supervisor in a brick form.

Concept is to put a particle (having slightly flat surface) on the flat surface of brick and then to tilt this brick by lifting it from one side at such an angle that the particle just starts to slide on the brick. The value of this angle can easily be measured by a protector. This angle is directly related to static coefficient of friction. The value of this measured angle is 30°.

From equation (10) value of static coefficient of friction can be evaluated by following procedure.
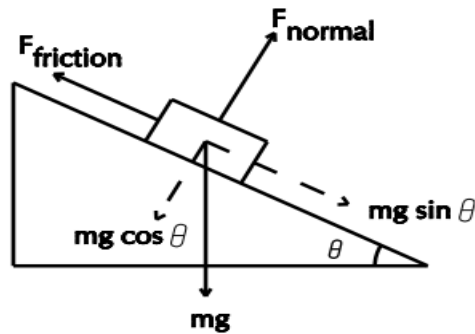
Figure 9: forces on a box on a tilted surface

In above figure, forces on the boxes can be balanced if we assume that θ is such an angle, that the box will just start to slide down. Therefore,

$$F_{normal} = mg \cos \theta \quad \& \quad F_{friction} = mg \sin \theta$$

Where $mg \cos\theta$ and $mg \sin\theta$ are two components of gravitational force mg. By substituting these values of normal and friction force in equation (10), we will get,

$$mg \sin \theta = \mu \, mg \cos \theta$$

$$\mu = \tan \theta \qquad\qquad (13)$$

By substituting $\theta = 30^0$ in equation (13) we will get, μ = 0.577.

6. Simulations with Rotating Kiln

After evaluating necessary parameters to account particle-particle and particle-wall interaction, simulations to model heat transfer inside rotating kiln were started. For this simulation, I have chosen the basic kiln geometry from former university student, who has done research on similar subject "Investigation of the particle movement in rotary kiln" (Ronzon, 2018). Below is the 2D illustrative diagram of kiln geometry.
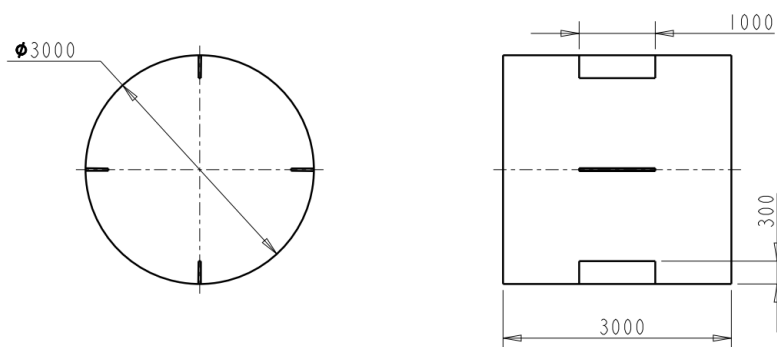
Figure 10: Illustrative diagram of kiln

This geometry has the following dimensional criteria:

Length of kiln: 3 m
Diameter of kiln: 3 m
Kiln inclination angle: 5º
Length of baffles: 1 m
Thickness of baffles: 30 mm

In this setup hot air is passed through one side and cold particles are injected from other side. Due to gravitational force and inclination and rotation of kiln, these particles will travel to the other side, where their temperature will be evaluated. The average time taken for a particle to reach from one side to other side will be measured as mean residence time.

Meshing in this geometry is done with hexahedral element shape, where maximum number of elements is 81379 and mesh has 7.50818e-01 minimum orthogonal quality.
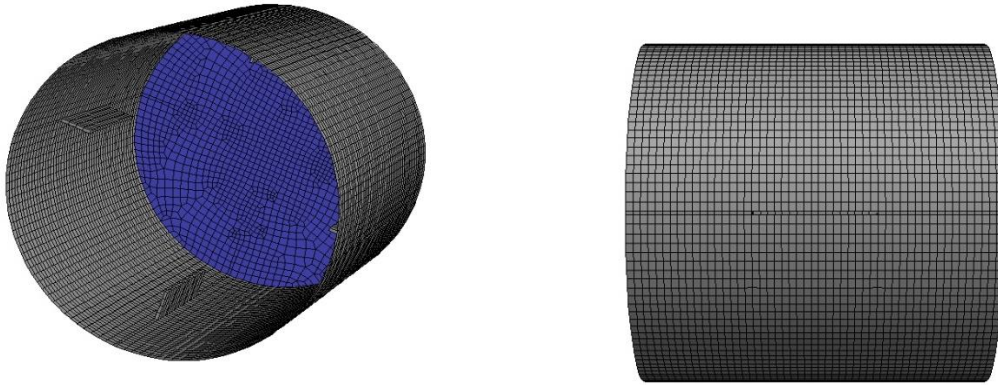
6.1 Setting up the Fluent

Physics setup: for this simulation, Eularian multi-phase model was used with DEM enabled inside "Discrete Phase Model" settings to consider particle-particle interaction. To include a viscous model, k-ε turbulence model is used with enhanced near wall treatment enabled. For dispersed phase material, material density was changed to 453.16kg/m^3 which corresponds to the density of real particle, provided to me by my supervisor and is used in real kiln.

Particle tracking strategy: In this simulation, I have used unsteady particle tracking in particle treatment window where each particle movement calculation is advanced by a specific number of particle time steps (it is not necessary that the particle has reached its final destination), before the flow solution is updated. Different time steps have been used for particle and flow as recommended by ANSYS for DEM.

Injection: For dispersed flow, in injection tab, we describe that when, where and how particle to be injected into the system. ANSYS Fluent offers various methods of injection for example, single, group, cone, surface, etc. In this simulation, group injection is used with 6 number of streams. Other injection data are as described below:

Particle type:	inert
Temperature:	300 K
Diameter distribution:	linear
Diameter:	0.001m to 0.012 m
Flow rate:	0.5 kg/s

Start time:	5 s
Stop time:	1000 s

DEM collision: It is necessary to insert data to model particle collisions, some of which have been evaluated in this study.

Normal contact force law:	spring-dashpot
Tangential contact force law:	friction-dshf
Spring-dashpot: k (N/m):	100
Spring-dashpot: eta:	0.111
Friction-dshf: mu-stick:	0.577
Friction-dshf: mu-glide:	0.4
Friction-dshf: mu-limit:	0.1
Friction-dshf: vel-glide (m/s):	1
Friction-dshf: vel-limit (m/s):	10
Friction-dshf: slope-limit (m/s):	100

Cell zone and boundary conditions: In cell zone condition, mesh motion was enabled to account for the rotation of kiln. For boundary conditions, as described earlier, hot gas with temperature of 400K is inserted into kiln with 3.7m/s velocity from one side and escapes from the other side at atmospheric pressure (0-gauge pressure). At the outlet side of particles, it is required to set "Discrete Phase Boundary Condition Type" to "escape" to make sure that particles do not remain inside the kiln after reaching to the other side.

Due to time limit and lack of computational power, time step size for fluid flow is set as 0.005s instead of 0.00075s and time step size for particle track is set as 0.0005s instead of $7.5*10^{-5}$ as evaluated in this study. To take into account the 5° of inclination of kiln, gravity is set to -9.7727 (m/s^2) in Y-direction and -0.855 (m/s^2) in Z-direction (Ronzon, 2018).

6.2 Simulation Result

This simulation was carried out for 120 s of real simulated time and result (summary file) was exported at every 30 s of simulated time. In this summary file, balancing parameters like number of particles inside fluid domain, particles which have escaped the domain, mass balance, energy balance etc. are stored. In below figures, particle position after 120 s time has been illustrated. Different figures represent respectively particle temperature, velocity and particle diameter. Notice the particle size distribution.
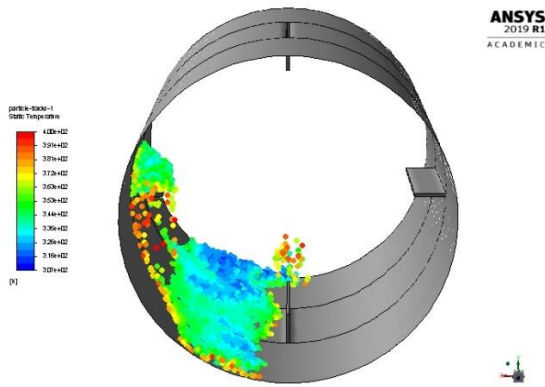
Figure 12: Particles colored by velocity of particles   *Figure 13: Particles colored by temperature of particles*
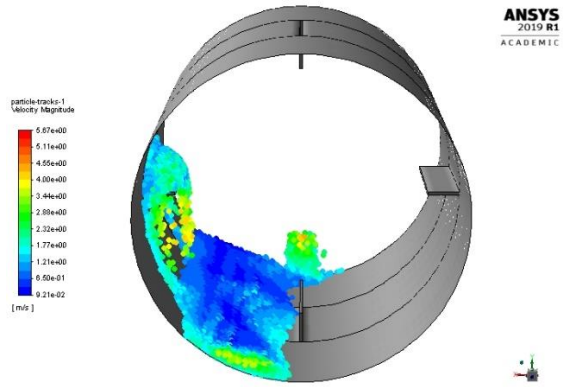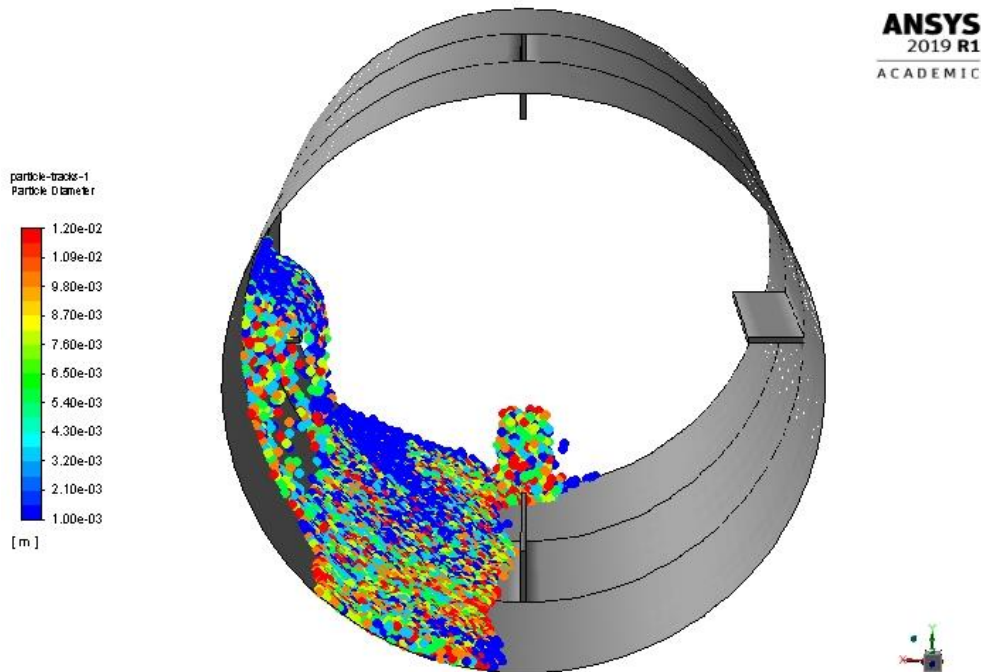
Figure 14: Particles colored by Particle diameter

As described earlier, Fluent DPM injects particles in parcels to make particle tracking easier. Therefore, if we want to calculate real number of particles and mass of real particles, then it can be calculated from mass transfer summary inside this dpm-summary file. In this output summary file, following result related to mass balance can be seen.

```
Fate                     Number              Elapsed Time (s)
Injection, Index
                                         Min        Max        Avg     Std Dev
Min                      Max
 ----                     ------  ---------- ---------- ---------- ----------
-------------------- --------------------
 in Fluid                 35500   5.000e-03  1.199e+02  1.791e+01  1.568e+01
injection-0 143994    injection-0   66
 Escaped - Zone 11        108500  1.365e+01  1.152e+02  2.699e+01  9.814e+00
injection-0 90562     injection-0 1386
 ----                     ------
 Net                      144000
 Injected                 144000

                    (*)- Mass Transfer Summary -(*)

 Fate                             Mass (kg)
                          Initial      Final     Change
 ----                    ---------- ---------- ----------
 in Fluid                8.875e+01  8.875e+01  0.000e+00
 Escaped - Zone 11       2.712e+02  2.712e+02  0.000e+00
 ----                    ---------- ---------- ----------
 Net                     3.600e+02  3.600e+02  0.000e+00
 Injected                3.600e+02
```

From this data, to calculate number of real particles from parcels following equation can be used,

$$N_p = \frac{m_p/\rho_p}{\pi d^3/6} \tag{14}$$

Calculation for real number of particles is important because, it is necessary to evaluate heat transfer coefficient.

6.3 Evaluation of heat transfer coefficient

In "Energy Transfer Summary" section of summary file, initial and final energy of particles in fluid and particles which have escaped the fluid domain is collected.

```
                    (*)- Energy Transfer Summary -(*)

          Fate                          Energy (J)
                                 Initial      Final     Change
          ----                  ---------- ---------- ----------
          in Fluid              2.758e+05  2.571e+06  2.295e+06
          Escaped - Zone 11     8.430e+05  1.184e+07  1.100e+07
          ----                  ---------- ---------- ----------
          Net                   1.119e+06  1.441e+07  1.329e+07
                  Injected                 1.119e+06
```

As shown in above data, change in energy of particles escaped the fluid domain is 1.100e+07 J. Inlet temperature of particles is pre-defined (300 K). To calculate outlet temperature of particles, following equation can be used:

$$\dot{Q} = \dot{m}_p c_p (T_{out} - T_{in}) \tag{15}$$

Where, $\dot{Q}$ will be 1.100e+07 J/s. Here, mass flow rate is the flow rate of particles escaping the fluid domain which will be different than mass flow rate of particle at injection which is 0.5kg/s. Value of $\dot{m}_p$ can be calculated by dividing total mass escaped from the domain to the mean residence time (average time taken by particles to escape the domain after being injected). Calculated value of $\dot{m}_p$ is 10.05 kg/s. Now, $\dot{Q}$ can be equated to Newton's equation of heat transfer,

$$\dot{Q} = \alpha S_p \Delta T_{ln} \tag{16}$$

Where, ΔT_{ln} is logarithmic mean temperature difference and S_p is total surface are of particles which have escaped the fluid domain. These two parameters can be calculated by following equation

$$\Delta T_{ln} = \frac{(T_f - T_{in}) - (T_f - T_{out})}{\ln{(T_f - T_{in})/(T_f - T_{out})}} \qquad \& \qquad S_p = N_p \pi d^2{}_p$$

As, we have value of $\dot{Q}, S_p$ and ΔT_{ln}, we can easily calculate the value of heat transfer coefficient α. Thus, heat transfer coefficient was calculated at time 30s, 60s, 90s and 120s with the help of a MATLAB script. Below is the table comparing the value of heat transfer coefficient at different time.

Time [s]	Mean residence time [s]	α [W/m²K]	T_{out} [K]
30	20.32	11.97	325.543
60	24.22	9.07	323.393
90	25.97	8.62	323.763
120	26.99	8.44	324.143

Table 8: Change in mean resident time and heat transfer coefficient with time

These values of mean residence time and heat transfer coefficient can be plotted against time to get better understanding of heat transfer process. But notice that, the output temperature of particles is almost same, and it will not change with the increase in simulation time substantially.
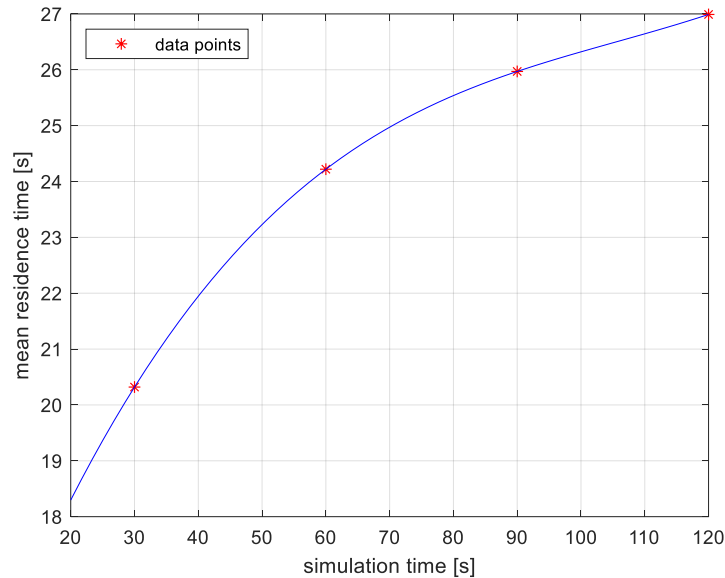
Figure 15: Graph of mean residence time v/s simulation time

In above graph, notice the time dependency of mean residence time. In the beginning of simulation, residence time is smaller and then it gradually increases. This happened because of increase in number of particles.

Mass flow rate of particle injection is constant through the time course. At the beginning, number of particles inside kiln is small. Therefore, particle-particle collisions are less, and the intensity of average forces exerted on each particle is less. Because of that, the movement of particle from one side to other side is faster. But, as the mass flow rate is constant, number of particles at an instance of time inside kiln increases. This leads to more particle-particle collisions and the intensity of average forces on each particle increases. As a result, it takes more time for particles to reach to the other side and mean residence time of particle increases. But, once the number of particles reaches to a constant value (number of injected particles = number of escaped particles), mean residence time will also approach to a constant value. Same reason can be applied to change in heat transfer coefficient, where it gradually decreases to reach a stable value.

The extrapolated value for mean residence time can be calculated as it was done in previous sections, where the time step was analyzed. But here, more important is the extrapolated value of heat transfer coefficient, which can be used to compare with performance change of kiln with change in air velocity and angular velocity of kiln.
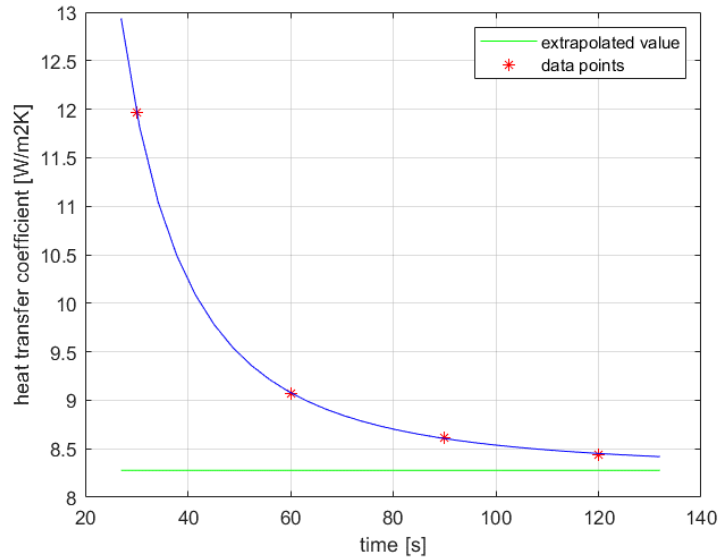
Figure 16: Graph of heat transfer coefficient v/s time

In the above graph, it is clear that value of α at time 120 s is close to extrapolated value of α. From the same calculation which is done in previous sections, it is found out that extrapolated value of α is 8.278 W/m²K and error is 2.00%. Hence, for further calculations and comparisons value of heat transfer coefficient is taken after 120 s of real time simulation for rotational speed of kiln N = 5RPM. For smaller rotational speed, it was increased to 210 s (N = 1.5 RPM) and 240 s (N = 0.5 RPM).

I have also performed one simulation with combination of K = 100 N/m and v = 0.992 for particle-particle interaction force law. But, from the output data, it was found out that the particles inside the kiln were more reflecting and jumping as seen in figure 18.
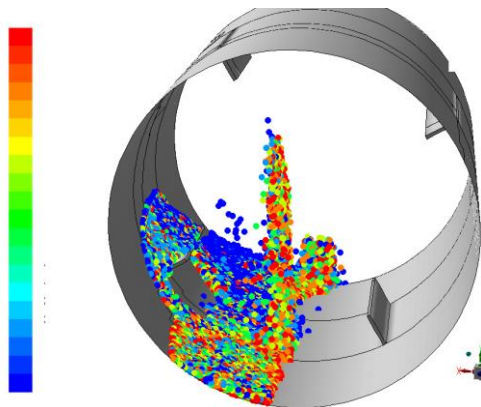
Figure 17: K = 100 N/m and v = 0.1
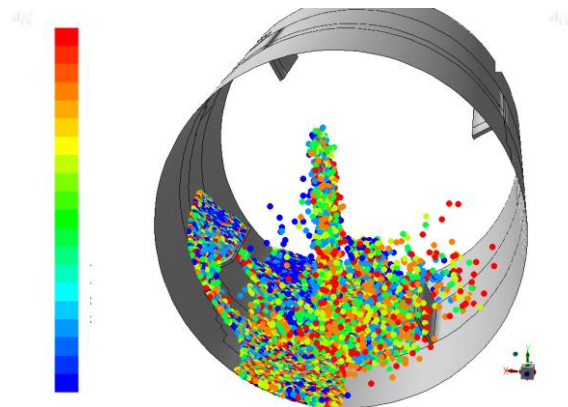
Figure 18: K = 100 N/m and v = 0.992

Above both pictures are taken after 50 s of real simulated time. But it is easily visible in figure 18 that, the particles have unusual behavior and they are jumping more that they should.

The calculated value of heat transfer coefficient is 9.37 W/m^{2}K with 4% of error with respect to the extrapolated value (9.01 W/m^{2}K), which is slightly higher than the one with the previous combination of spring constant and restitution coefficient. This can be explained that due to unusual jumping of particle more surface area of particles come into contact with hot gas which results into more heat transfer (and also turbulence in gas). In appendix, I have attached table and graph comparing particle residence time and heat transfer coefficient with simulated time.

At this moment, I am unable to state the reason for such unusual behavior of particles. Because of this reason and limited time, further simulations are carried out with K = 100 N/m and ν = 0.111.

7. Nusselt Correlation

As we all know that the Nusselt number is the ratio of convective heat transfer to the conductive heat transfer across a boundary of the given system.

$$\text{Nu} = \frac{\alpha L_{char}}{\lambda}$$

Inside of a kiln, if both continuous phase and discrete phase is steady then, the heat transfer between these phases will mainly occur due to conductive heat transfer. Since air is continuous phase here, the effect of heat transfer will be very negligible. But that is not the case here. Both continuous phase and discrete phase are in motion. Therefore, effect of heat transfer will largely be affected by relative motion of continuous phase because of eddies and turbulence. So, if I can somehow evaluate the relation between Nusselt number and Reynolds number, it will be easy to understand the effect of fluid motion on heat transfer.

7.1 Evaluation of Empirical Equation

Many empirical equations have been derived for Nusselt number in different studies in the form of

$$\text{Nu} = f(\text{Re}, \text{Pr})$$

$$\text{Where, } \text{Re} = \frac{\rho u_g L_{char}}{\mu_l} \quad \& \quad \text{Pr} = \frac{u_g}{a}$$

$$\text{Thermal diffusivity, } a = \frac{\lambda}{\rho c_{pg}}$$

Dittus-Boelter correlation (Dittus and Boelter, 1930) is one of the well-known empirical equations, which gives the relation between Nusselt number and Reynolds number for a fully developed turbulent flow through pipe.

$$\text{Nu} = 0.023 \text{Re}^{0.8} \text{Pr}^{\frac{1}{3}} \tag{17}$$

To evaluate similar empirical correlation, more simulations were performed with different velocity of air but same inlet temperature. Dependency of Nusselt number and Reynolds number on air inlet velocity can be seen in the table below.

u_g [m/s]	t_m [s]	α [W/m²K]	Nu	Re
0.1	21.35	4.37	1.1728	44.498
0.2	21.45	5.37	1.3393	88.996
0.4	21.65	5.48	1.4724	177.992
1	22.34	6.12	1.6437	444.982
2	23.72	7.21	1.9367	889.963
3	25.35	7.90	2.1229	1334.944
3.7	26.99	8.44	2.2680	1646.431

Table 9: velocity dependency of tm, α, Nu and Re (N = 5 RPM and $L_{char} = d_p = 6.5\ mm$)

In the table we can see that value of Nusselt number, Reynolds number and as a result of that, heat transfer coefficient increases with increase in inlet air velocity. Which is logical because with increase in air velocity turbulence and eddies will increase, which is responsible for convective heat transfer.

This data can be used to evaluate a new empirical equation with two unknown variables,

$$\text{Nu} = C_1 \text{Re}^{C_2} \text{Pr}^{\frac{1}{3}} \tag{18}$$

which will be similar to Dittus-Boelter correlation (Dittus et al, 1930). The value of unknowns C_1 and C_2 can be evaluated by non-linear regression. MATLAB software offers a function for non-linear regression analysis called "`nlinfit`" which evaluates the unknown parameters of the given function from input data. From this calculation, the evaluated value of unknown variables with rotational speed of kiln as 5 RPM and characteristic length as average particle diameter (6.5 mm) is,

$$C_1 = 0.663 \pm 0.1455$$
$$C_2 = 0.175 \pm 0.0339$$

Substituting these values in equation (18) we will get following empirical equation for relation between Nusselt number and Reynolds number for heat transfer between air and solid particles inside rotating kiln.

$$\text{Nu} = 0.663 \text{Re}^{0.175} \text{Pr}^{\frac{1}{3}} \tag{19}$$

There is another empirical Nusselt correlation for heat transfer for fluid flowing around a sphere (Bird at al, 2007)

$$Nu = 2.0 + \left(0.4\text{Re}^{\frac{1}{2}} + 0.06\text{Re}^{\frac{1}{2}}\right)\text{Pr}^{\frac{1}{3}} \quad , \quad 3.6 < \text{Re} < 7.6\text{x}10^4 \qquad (20)$$

If I plot a logarithmic graph of Nusselt correlation from equation (19) and (20), it can show us the similarity (if there is any) between these correlations.
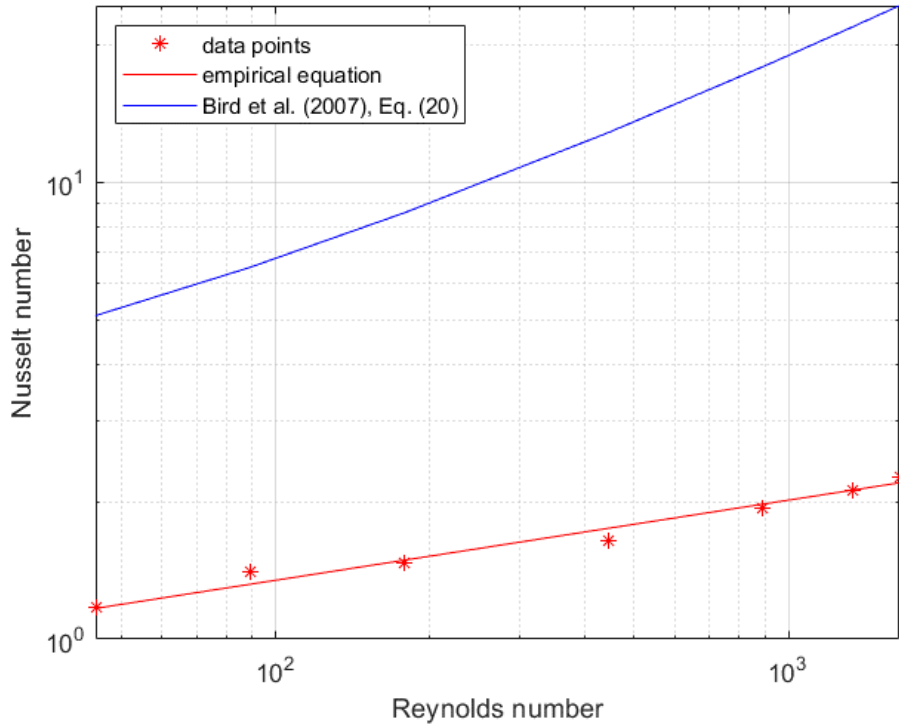
Figure 19: comparison of two different Nusselt correlation

In above graph, notice that shape of both the curves is similar but magnitude of Nusselt number is different. There is also big difference in exponent of Re for Dittus-Boelter correlation (0.8) and my correlation. This dissimilarity can be explained if the effect of gas velocity does not have a large impact while the effect of rotational speed of kiln might have greater impact.

To inspect the effect of rotational speed of kiln on heat transfer between phases more simulations were carried out with different kiln rotation speed.

7.2 Effect of Rotational Speed of Kiln

Simulations were performed with combination of three different rotational speed of kiln, N = 0.5, 1.5, 5 RPM (N = 5 RPM had been discussed in previous section) and different inlet velocity of air. In below tables, simulation results for N = 0.5 RPM and 1.5 RPM have been illustrated. In both the cases, the characteristic length in Reynolds number as well as Nusselt number was equal to the average diameter of particles.

N = 0.5RPM

u_g [m/s]	t_m [s]	α [W/m^{2}K]	Nu	Re
0.1	77.69	0.39	0.1057	44.498
0.25	77.66	0.49	0.1307	111.245
0.6	77.73	0.65	0.1747	266.989
1.5	78.71	1.16	0.3109	667.472
3.7	82.75	2.47	0.6627	1646.432

Table 10: velocity dependency of tm, α, Nu and Re for N=0.5 RPM

Figure 20: Nusselt correlation comparison for N = 0.5RPM

For this case, C_1 and C_2 in Nusselt correlation are evaluated by non-linear regression as follow:

$$C_1 = 0.00477 \pm 0.00879$$
$$C_2 = 0.675 \pm 0.2605$$

This gives Nusselt empirical equation as, $\mathrm{Nu} = 0.0048 \mathrm{Re}^{0.675} \mathrm{Pr}^{1/3}$.

N = 1.5RPM

v_g	t_m	α	Nu	Re
0.1	48.69	1.01	0.2704	44.498
0.25	48.85	1.26	0.3374	111.245
0.6	49.0	1.51	0.4056	266.989
1.5	50.12	2.08	0.5590	667.472
3.7	55.38	3.70	0.9945	1646.432

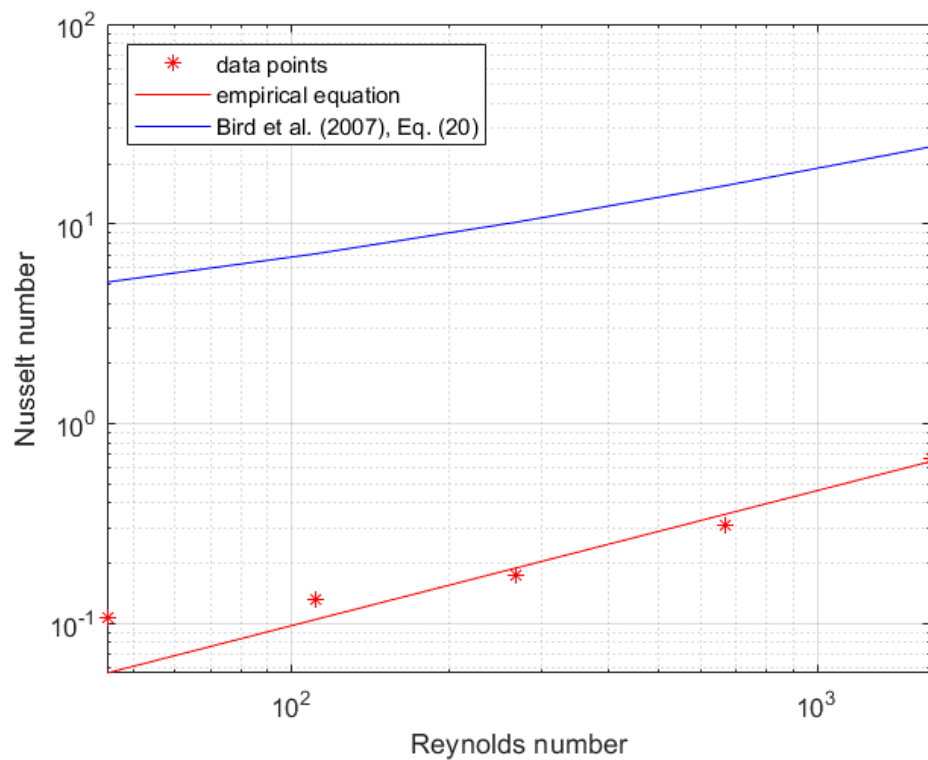*Table 11: velocity dependency of tm, α, Nu and Re for N=1.5 RPM*
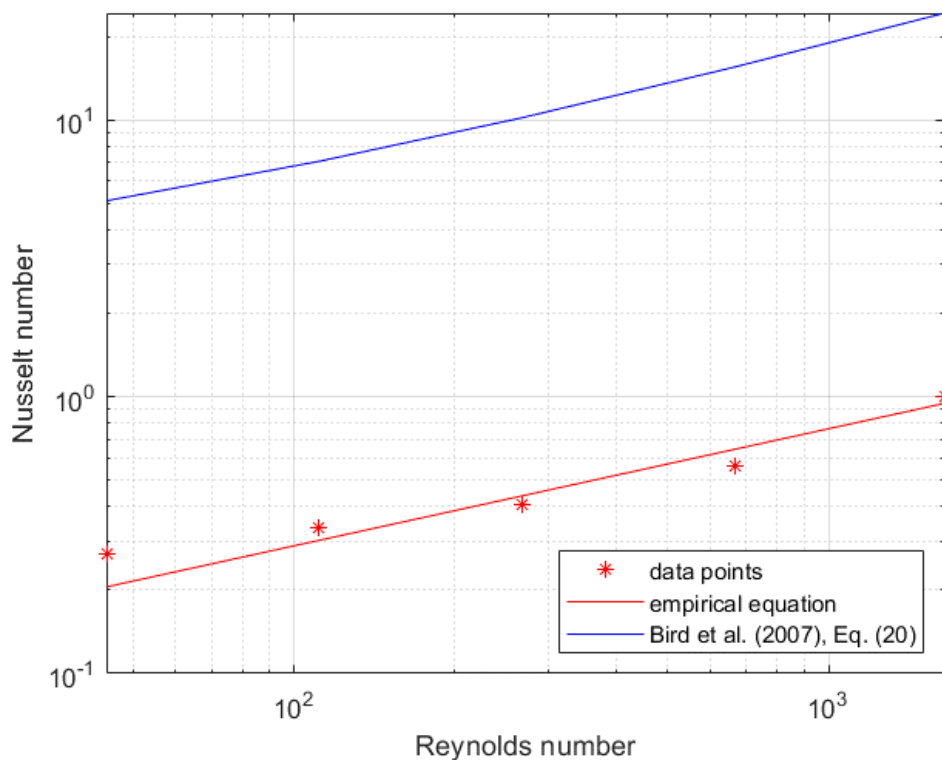
Figure 21: Nusselt correlation comparison for N = 1.5RPM

For this case, C_1 and C_2 in Nusselt correlation are evaluated by non-linear regression as follow:

$$C_1 = 0.04558 \pm 0.06104$$
$$C_2 = 0.423 \pm 0.1974$$

This gives Nusselt empirical equation as, $\mathrm{Nu} = 0.0456\mathrm{Re}^{0.423}\mathrm{Pr}^{1/3}$.

In above simulation data, notice the air velocity dependency on heat transfer coefficient for both the rotational speed. Changing the air velocity from 0.1 to 3.7m/s does not have as much effect as changing the rotational speed from 0.5 to 1.5 and 5RPM. This proves my previous assumption for having different exponents for Re

that rotational speed of kiln has bigger impact on heat transfer between phases than air velocity and exponent of Re should differ for Dittus-Boelter correlation and my correlation as Dittus-Boelter correlation is for a flow through duct where, velocity of fluid is the only one variable to form turbulence.

In the above calculations of the Nusselt correlations, average diameter of particle (6.5 mm) was used as the characteristic length. But, Similar Nusselt correlations can be evaluated by using diameter of kiln as characteristic length. This change should be visible only in the leading constant C_1, exponents of the Reynolds number should stay same.

N = 0.5 RPM and $L_{char} = D$

$$\text{Nu} = 0.0035\text{Re}^{0.675}\text{Pr}^{1/3} \quad \text{where,} \quad \begin{aligned} C_1 &= 0.03487 \pm 0.11982 \\ C_2 &= 0.675 \pm 0.2605 \end{aligned}$$
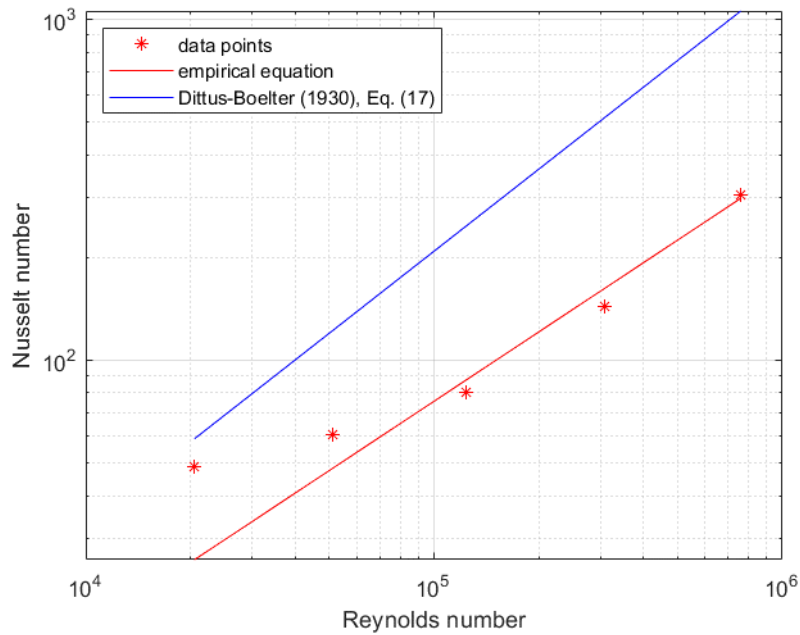
Figure22: Nusselt correlation for N = 0.5 RPM and L_{char}= D

N = 1.5 RPM and $L_{char} = D$

$$\text{Nu} = 1.573\text{Re}^{0.423}\text{Pr}^{1/3} \quad \text{where,} \quad \begin{aligned} C_1 &= 1.57297 \pm 4.00177 \\ C_2 &= 0.423 \pm 0.1974 \end{aligned}$$

43
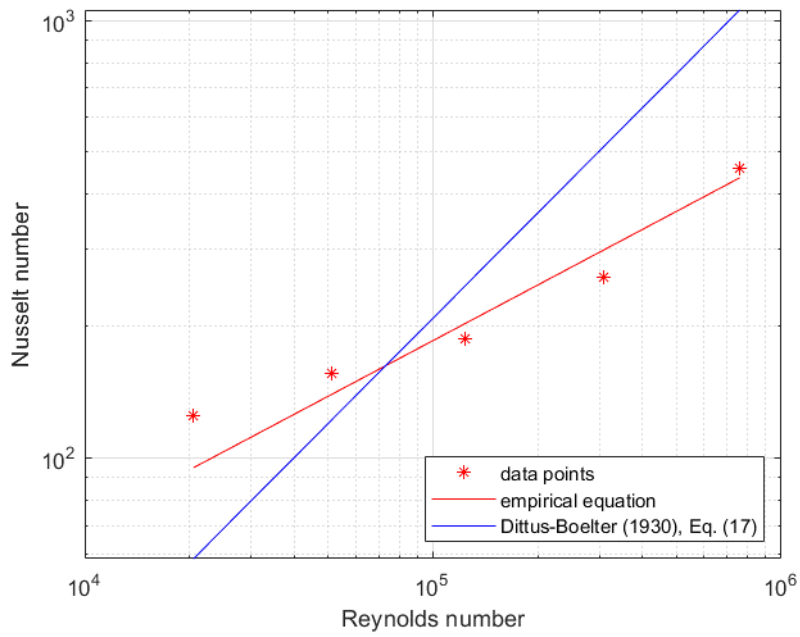
Figure 23: Nusselt correlation for N = 1.5 RPM and L_{char} = D

N = 5 RPM and $L_{char} = D$

$$\text{Nu} = 104.5\text{Re}^{0.175}\text{Pr}^{1/3} \qquad \text{where,} \qquad \begin{array}{l} C_1 = 104.501 \pm 44.5277 \\ C_2 = 0.175 \pm 0.0339 \end{array}$$
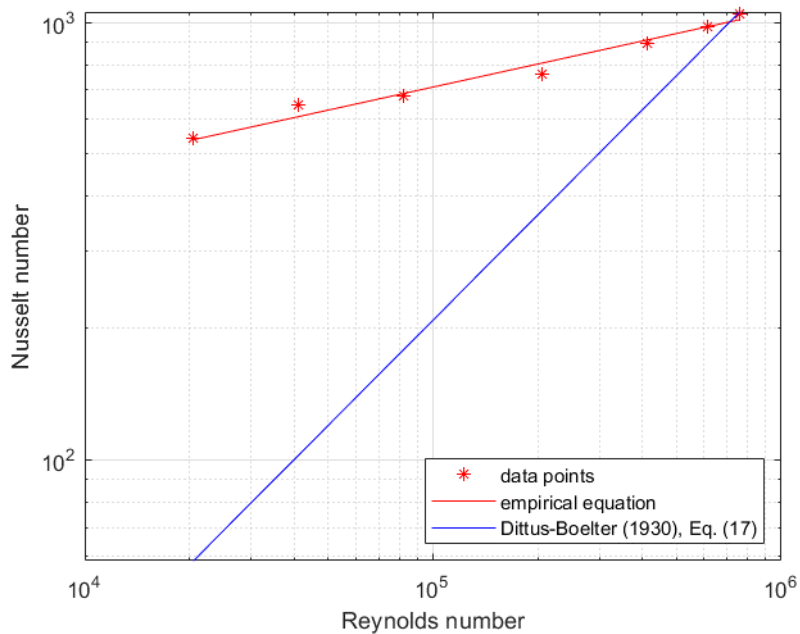

Figure 24: Nusselt correlation for N = 5 RPM and L_{char} = D

For ease of readability, I have added a table of these Nusselt correlation corresponding to their characters length and rotational speed below.

	N = 0.5 RPM	$Nu = 0.0048 Re^{0.675} Pr^{1/3}$
$L_{char} = d_p$	N = 1.5 RPM	$Nu = 0.0456 Re^{0.423} Pr^{1/3}$
	N = 5.0 RPM	$Nu = 0.663 Re^{0.175} Pr^{1/3}$
	N = 0.5 RPM	$Nu = 0.0035 Re^{0.675} Pr^{1/3}$
$L_{char} = D$	N = 1.5 RPM	$Nu = 1.573 Re^{0.423} Pr^{1/3}$
	N = 5.0 RPM	$Nu = 104.5 Re^{0.175} Pr^{1/3}$

Table 12: Nusselt correlation corresponding to their characteristic length and kiln rotational speed

As we can see in the table above, correlation for different characteristic length differs in leading constant C_1 only.

7.3 Nusselt Correlation to Include Rotational Speed

In previous subsection, I concluded that, coefficient and exponent of Re will change with change in rotational speed. But, if I somehow evaluate an empirical relation that includes both air velocity and angular velocity of kiln, then we don't need to evaluate the exponent coefficient of Re each time. Concept is to somehow combine Nusselt correlation with Reynolds number for air velocity and Reynolds number for rotational speed of kiln. This correlation may look like,

$$Nu = C_1 \, Re_g^{C_2} \, Re_N^{C_3} \, Pr^{\frac{1}{3}} \tag{21}$$

where, Re_g represents Reynolds number for air velocity and Re_N represents Reynolds number for rotational speed of kiln. The relation between rotational speed and circumferential velocity is given by,

$$u \propto DN$$

Where, D is the diameter of kiln and N is the rotational speed of kiln in RPS. This give Reynolds number for rotational speed as,

$$Re_N = \frac{N L_{char} D}{\nu} = \frac{N D^2}{\nu}$$

Here, in definition of Nu and Re, characteristic length is taken as kiln diameter. It would make more sense to use this diameter as characteristic length as I am trying

to evaluate correlation for Nusselt number and Reynolds number corresponding to kiln rotation. In the table below, there is a dependency of Nu on Re_N and Re_g.

	v [m/s]	Re_g	Re_N	Nu
N = 0.5 RPM	0.1	20537	5134	48.78
	0.25	51344	5134	60.30
	0.6	123225	5134	80.65
	1.5	308064	5134	143.48
	3.7	759891	5134	305.85
N = 1.5 RPM	0.1	20537	15403	124.79
	0.25	51344	15403	155.71
	0.6	123225	15403	187.21
	1.5	308064	15403	258.01
	3.7	759891	15403	459.04
N = 5 RPM	0.1	20537	51344	541.28
	0.2	41075	51344	645.83
	0.4	82150	51344	679.57
	1.0	205376	51344	758.63
	2.0	410752	51344	893.84
	3.0	616128	51344	979.80
	3.7	759891	51344	1046.75

Table 13: dependency of Nu on Re_N and Re_g

From the non-linear regression, the values of C_1, C_2 and C_3 are as follow:

$$C_1 = 0.00921 \pm 0.0159$$
$$C_2 = 0.19963 \pm 0.0558$$
$$C_3 = 0.83214 \pm 0.1511$$

From these values, empirical equation for Nusselt number will be,

$$Nu = 0.009 \, Re_g^{0.2} \, Re_N^{0.832} \, Pr^{\frac{1}{3}} \tag{22}$$

This equation can be rearranged to plot a 2D chart by,

$$\frac{\text{Nu}}{Pr^{\frac{1}{3}}\text{Re}_N^{0.832}} = 0.009Re_g^{0.2} \tag{23}$$

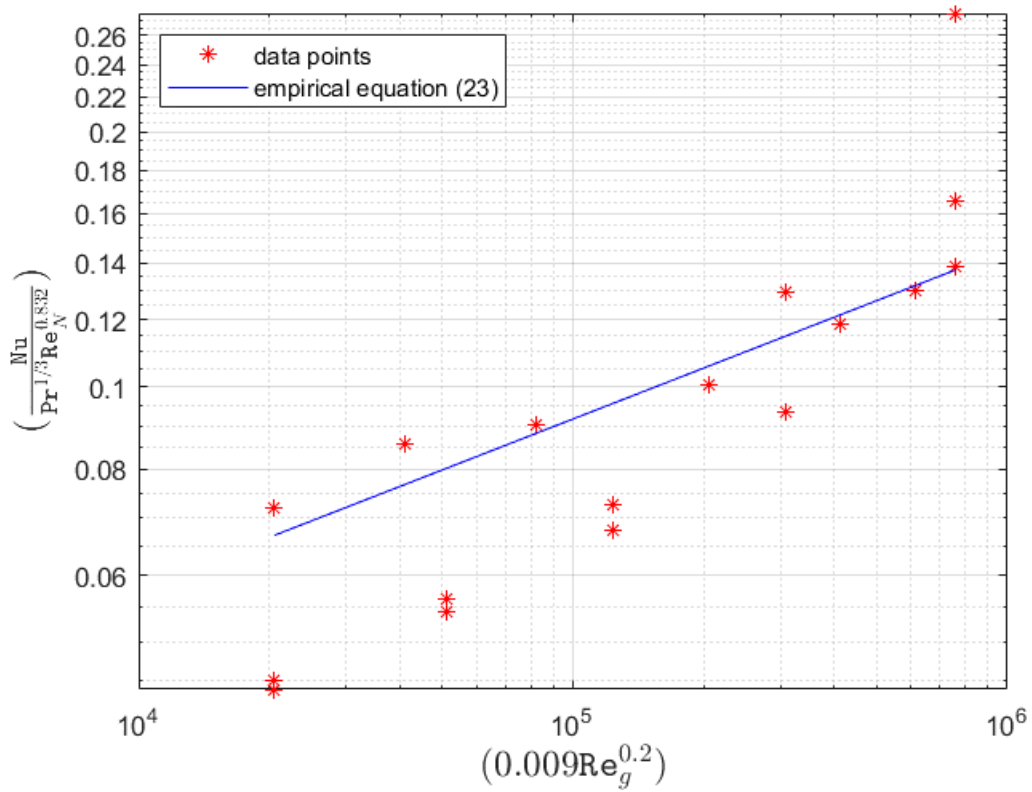where the left hand side corresponds to values on vertical axis of the following figure.

Figure 25: dependency of Nu on Re_N and Re_g

8. Conclusion

In this study, simulations for multiphase flow have been carried out in ANSYS Fluent where, one phase is dispersed phase and other one is continuous phase. Continuous phase was modeled in Eularian frame of reference and dispersed phase was modeled in Lagrangian frame of reference. For Lagrangian frame of reference, in ANSYS Fluent, there are two modelling strategies to contemplate particle-particle interactions: Kinetic Theory of Granular Flow (KTGF) and Discrete Element Method (DEM). Following parameters concerning these two modelling methods were evaluated.

Size of ideal time step: From the convergency index, it was proved that, when using KTGF model for particle-particle interaction, ideal time step is 0.008 s and for DEM, it is 0.000075 s. This big difference in time step size will greatly affect the selection of one of these methods when, simulating dense dispersed flow as it will increase the total simulation time by approximately 10 times.

Coefficient of restitution and spring constant: In KTGF method, forces due to particle-particle are transferred to other particles by coefficient of restitution and in DEM method, spring constant is utilized along with restitution coefficient. For KTGF value of restitution coefficient for given particle material was determined in the experiment as 0.3936. On the other hand, for DEM there are combinations of spring constant and restitution coefficient where, for one value of spring constant, there are two value of restitution coefficient that give the same particle reflection. All the consequent simulations used combination of K = 100 N/m and restitution coefficient 0.111 fitted on the experimental results.

Heat transfer inside rotating kiln between gas and solid particles: At the beginning of the process, heat transfer coefficient is higher and then it gradually decreases with time but, the mean residence time gradually increases because the number of particles inside kiln will increase till the mass flow rate of injected particles and the mass flow rate of escaped particles becomes same.

Nusselt correlation for heat transfer: From the results of simulations, it was proved that velocity of gas inside kiln does not have as great impact as angular velocity of kiln. As a result of that, various Nusselt-Reynolds correlations were evaluated similar to the Dittus-Boelter correlation with different coefficient and exponent of Reynolds number.

9. Proposition for Future Work

Even though some prominent results were obtained in this study, for heat transfer coefficient evaluation, basic geometry of kiln was used. Further work can be done with different size and type of kiln and also using different shapes and numbers of baffles inside kiln.

As concluded earlier that in DEM there are two values of coefficient of restitution for given spring constant that gives same particle reflection, but in the simulations, while using combination of K = 100 N/m and ν = 0.992, it was found out that intensity of forces on particle due to particle-particle interactions is higher than it should be. Therefore, particles were more reflecting and jumping. I am unable to explain the reason for this kind of behavior of particles at this moment. In future, more research can be done subjecting this issue and such behavior of particles can be explained.

While running simulation with DDPM-KTGF method, I was getting error after some simulated time. Reason for this error is unknown. Even though it is recommended by ANSYS software distributor in Czech Republic to use DEM method for such simulations, using DDPM-KTGF method can help reduce time take to run a simulation by approximately 10 times. Hence, it would be great if some way can be worked out in future research to avoid this error.

10. List of Symbols

Name	Symbol	Unit
Volume fraction of dispersed phase	α_d	-
Volume fraction of continuous phase	α_q	-
Density of dispersed phase	ρ_d	-
Velocity of dispersed phase	u_d	-
Time	t	-
Velocity of continuous phase	u_q	-
Thermodynamic pressure	p	Pa
Solid pressure	p_d	Pa
Stress tensor for dispersed phase	$\overrightarrow{\tau_d}$	Pa
Gravitational acceleration	g	(m/s^2)
Interphase drag coefficient	β	-
Virtual mass force	F_{vm}	N
Lift force	F_{lf}	N
Spring-dashpot force	$\vec{F}_\delta$	N
Spring constant	K	N/m
Overlap during particle collision (DEM)	δ	m
Unit vector	$\bar{e}$	-
Coefficient of restitution	ν	-
Coefficient of static friction	μ	-
Damping coefficient	γ	kg/s
Dynamic viscosity of liquid	μ_l	Pas
Particle energy rate	$\dot{Q}$	J/s
Particle mass flow rate	$\dot{m}_p$	kg/s
Specific heat of particle material	c_p	J/kgK
Coefficient of heat transfer	α	W/m²K

Total surface area of particles	S_p	m²
Logarithmic temperature difference	ΔT_{ln}	K
Temperature of air	T_f	K
Temperature of injected particles	T_{in}	K
Temperature of escaped particles	T_{out}	K
Mean residence time	t_m	s
Diameter of particle	d_p	m
Conductive heat transfer coefficient	λ	W/mK
Thermal diffusivity	a	m²/s
Kinematic viscosity of air	u_g	m²/s
Characteristic length	L_{char}	m
Specific heat of air	c_{pg}	J/kgK
Velocity of air inside kiln	$\mathbf{v}_g$	m/s
Diameter of kiln	D	m

REFERENCES

- Besnard, D.C., Harlow, F.H. (1988) "Turbulence in multiphase flow", International Journal of Multiphase Flow, Volume 14, Issue 6, Pages 679-699.

- Bird, R. B., Stewart, W. E., Lightfoot, E. N. (2007) Transport Phenomena, John Wiley and Sons, Inc., New York, USA pages 905

- Branco, A. M. C., Mesquita, A. L. A., Vaz, J. R. P. (2015) Application of the Linear Spring-Dashpot Model in the CFD-DEM Simulation of Alumina Fluidization, Universidade Federal do Pará, Belém, Pará, Brazil

- Celik, I., Chen, C.J., Roache, P.J., Scheurer G., eds (1993) Symposium on Quantification of Uncertainty in Computational Fluid Dynamics. FED-ASME, Vol. 158. New York: Am. Soc. Mech. Eng.

- Cundall, P. A., and Strack (1979) "A discrete numerical model for granular assemblies", Geotechnique, 29, pp. 47-65.

- Debashis, B., Kaushik, D., Kevin, S., Goodluck, O. (2015) Comparison of Eulerian-Granular and Discrete Element Models for Simulation of Proppant Flows in Fractured Reservoirs, Proceedings of the ASME 2015 International Mechanical Engineering Congress and Exposition, Houston, Texas, USA

- Ding, J., and Gidaspow, D. (1990) "A bubbling fluidization model using kinetic theory of granular flow", AIChE Journal, 36(4), pp. 523-538.

- Dittus, F.W. and Boelter, L.M.K. (1930) Heat Transfer in Automobile Radiators of the Tubular Type. Publications in Engineering, University of California, Berkeley, Vol. 2, 443.

- Franziska, G., Christoph, K., Thomas, F., Friederike, L., Lindner, S., Rudiger, S. (2016) Assessment of Particle-tracking Models for Dispersed Particle-laden Flows Implemented in OpenFOAM and ANSYS FLUENT, Engineering Applications of Computational Fluid Mechanics, 10:1, 30-43

- Gidaspow, D., Bezburuah, R., and Ding, J. (1992) "Hydrodynamics of circulating fluidized beds, kinetic theory approach", In Fluidization VII, Proceedings of the 7th Engineering Foundation Conference on Fluidization, pp. 75-92, Brisbane, Australia.

- Kozic, S., Ristic, M., Puharic, B., Katavic (2011) Comparison of Euler-Euler and Euler-Lagrange Approach in Numerical Simulation of Multiphase Flow in

Ventilation Mill-air Mixing Duct, Serbian Congress in Theoretical and Applied Mechanics-3, B-08.

- Liu, D., Bu, C., Chen, X. (2013) Development and Test of CFD-DEM Model for Complex Geometry: A Coupling Algorithm for Fluent and DEM. Comput. Chem. Eng. 58, 260–268.

- Pezo, M., Pezo, L., Jovanivic, A., Loncar, B., Colovic, R. (2016) DEM/CFD Approach for Modeling Granular Flow in the Revolving Static Mixer, Chemical Engineering Research and Design, Issue 109, pages 317-326.

- Ronzon, T. (2018) Investigation of the Particle Movement in Rotary Kiln, Czech Technical University in Prague

- Rota, G.C. (1964), "Reynolds operators", Proceedings of Symposia in Applied Mathematics, Vol. XVI, Providence, R.I.: Amer. Math. Soc., pp. 70–83, MR 0161140.

- Schaeffer, D.G. (1985) Instability in the Evolution Equations Describing Incompressible Granular Flow, Journal of Differential Equations, Issue 66, pages 19-50.

- Subramaniam, S. (2013). Lagrangian-Eulerian Methods for Multiphase Flows. Progress in Energy and Combustion Science, 39, 215–245.

- Syamlal, M., Rogers, W., and O'Brien, T. J. (1993) "MFIX documentation: Volume 1, Theory Guide. National Technical Information Service, Springfield, VA, DOE/METC-9411004, NTIS/DE9400087.

- Zhu, H., Zhou, Z., Yang, R., Yu, A. (2007) Discrete particle simulation of particulate systems: Theoretical developments. Chemical Engineering Science, Issue 62, Pages 3378–3396.

Appendix 1

Time dependence of mean residence time and heat transfer coefficient between hot gas and particles on real simulated time for DEM with K = 100 N/m and v = 0.992.

Time [s]	Mean residence time [s]	α [W/m²K]	T_{out} [K]
30	20.32	13.75	325.543
60	24.22	10.33	323.393
90	25.97	9.66	323.763
120	26.99	9.37	324.143
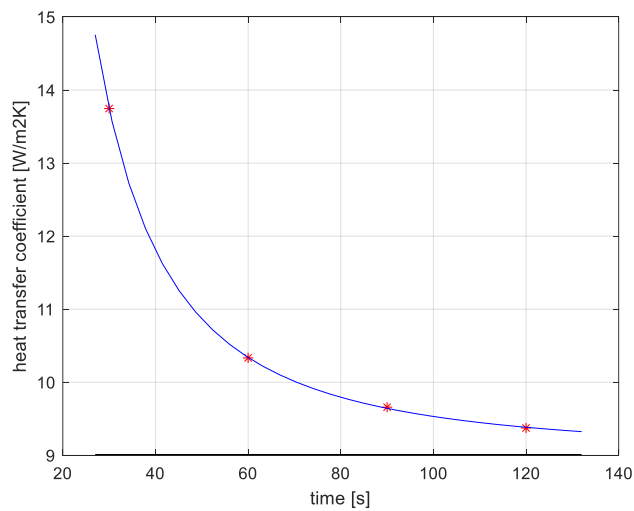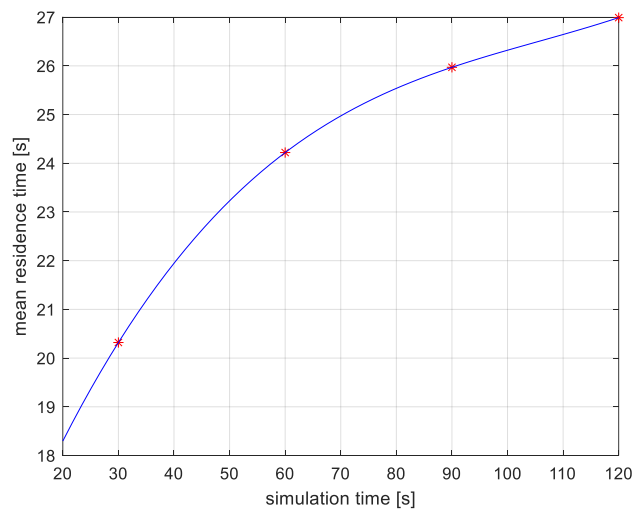
Appendix 2

MATLAB script to evaluate extrapolated value for give quantity

```matlab
t = [0.371734 0.3711145 0.374780 0.374707 0.374719 0.375677];
ymax =[0.016625 0.016788 0.018697 0.018654 0.018675 0.018576];
ts = [0.005 0.001 0.00075 0.000625 0.0005 0.00025];

figure(1)
plot(t,ts,'*');
figure(2)
tr = 1;
N = tr./ts;
plot(N,ymax,'*-');
% yy=smooth(ymax);
% plot(yy,ts)

i = [1, 2, 3];
i = [3, 4, 5];
i = [2, 3, 4];
N = N(i);
Phi = ymax(i);

[N, i] = sort(N,'descend');  % reverse order of elements so that the first
element represent the finest mesh
Phi = Phi(i);

figure(1);
plot(N,Phi,'r*', N,Phi,'b');
grid on;

D = 1;  % dimension of the problem, 2-D or 3-D

r21 = (N(1)/N(2))^(1/D)
r32 = (N(2)/N(3))^(1/D)
if ( r21 < 1.3 || r32 < 1.3 )
  disp('refinement factors r21 and r32 should be greater than 1.3');
end

eps32 = Phi(3)-Phi(2)
eps21 = Phi(2)-Phi(1)
R = eps21/eps32
s = sign(eps32/eps21)

fq = @(p) log((r21.^p-s)./(r32.^p-s));
fp = @(p) p - 1/log(r21)*abs(log(abs(eps32/eps21))+fq(p));
%p = fzero(fp,1)
p = fsolve(fp,1)

Phi21ext = (r21^p*Phi(1)-Phi(2))/(r21^p-1)
e21a = abs((Phi(1)-Phi(2))/Phi(1))*100
CGI21 = 1.25*e21a/(r21^p-1)

e32a = abs((Phi(2)-Phi(3))/Phi(2))*100
CGI32 = 1.25*e32a/(r32^p-1)

CGI33 = 1.25*abs(Phi21ext-Phi(3))/Phi(3)*100
```

Appendix 3

MATLAB script to evaluate coefficient and exponents of Re_N and Re_g by nonlinear regression

```matlab
% gas property
rho = 1.225;
mu = 1.7894e-05 ;
lambda = 0.0242;  % thermal conductivity
cp = 1006.43;
nu = mu/rho;
a = lambda/(rho*cp);
Pr = nu/a;
dp = 6.5e-3; %particle diameter
Lchar = dp;
D = 3;        %kiln diameter
Lchar = D

%% N=5

nu5 = [541.285564 645.831349 679.570012 758.633496 893.844846 979.806277
...
                                              1046.756966];
rey5 = [20537.610372 41075.220744 82150.441489 205376.103722 410752.207444
...
                                    616128.311166 759891.583771];
ReyN5 = 5*Lchar*D/nu/60*ones(1,length(rey5));
% v = [0.1 0.2 0.4  1 2 3 3.7];
% plot(v,rey)

%% N=0.5

nu05 = [48.786700 60.309200 80.651600 143.482000 305.857000];
rey05 = [20537.610372 51344.025930 123225.662233 308064.155583 ...
                                              759891.583771];
ReyN05 = 0.5*Lchar*D/nu/60*ones(1,length(rey05));

%% N=1.5

nu15 = [124.793266 155.713268 187.215404 258.016883 459.039154];
rey15 = [20537.610372 51344.025930 123225.662233 308064.155583 ...
                                              759891.583771];
ReyN15 = 1.5*Lchar*D/nu/60*ones(1,length(rey15));

%% non-linear regression
Yi = [nu05 nu15 nu5];  % value of Nu corresponding to Reyg and ...
                                              ...ReyN below
Reyg = [rey05 rey15 rey5];
ReyN = [ReyN05 ReyN15 ReyN5];
Xi = [Reyg; ReyN];

Xi = Xi';
Yi = Yi';

fmodel = @(b,x) b(1).*x(:,1).^b(2).*x(:,2).^b(3).*Pr^(1/3);

% nuss = 2.0+(0.4*Reyg.^(1/2) + 0.06*Reyg.^(2/3))*Pr^(1/3); % sphere
  p0 = [0.66 0.175 0.175];
```

```matlab
b = nlinfit(Xi,Yi,fmodel,p0)

Yin = Yi./(Pr^(1/3)*Xi(:,2).^b(3));
Xin = Xi(:,1);
y = fmodel(b,Xi)./(Pr^(1/3)*Xi(:,2).^b(3));
y2 = b(1)*Xin.^b(2);

loglog(Xin,Yin,'r*', Xin,y,'b');
legend('data points', 'empirical equation','location','northwest')
ylabel('${\it} (\frac{\tt{Nu}}{{\tt{Pr}}^{1/3}{\tt{Re}}_N^{0.832}})$',...
                    'interpreter','Latex','FontSize',14);
xlabel('${\it} (0.009{\tt Re}_{g}^{0.2})$','interpreter','Latex',...
                                        'FontSize',14);

grid on;
```